XV. PHYSICAL ELECTRONICS AND SURFACE PHYSICS[*]

Academic and Research Staff

Prof. R. E. Stickney
Dr. D. L. Fehrs
Dr. T. J. Lee

Graduate Students

J. C. Batty   L. J. Forney   T. Viswanathan
A. E. Dabiri   H. C. Juvkam-Wold   S. Yamamoto

RESEARCH OBJECTIVES AND SUMMARY OF RESEARCH

The general purpose of our research program is to study problems relating to the atomic, molecular, and electronic processes occurring at gas-solid interfaces. Examples of these processes are: thermionic emission, surface ionization, adsorption, absorption, oxidation, catalysis by metals, electrode processes in electrical discharges, and the scattering of molecular beams from solid surfaces. At present, we are concentrating on the following problems.

1. Adsorption of Gases and Vapors on Solid Surfaces

The objective of this study is to contribute to the development of a theory of adsorption of gases or vapors on solid surfaces. Our major effort has been directed toward obtaining experimental data on both the energy and dipole moment of the adsorption bond between the adsorbate and the substrate. The energy is determined from residence-time measurements based on a modulated molecular-beam technique, whereas the dipole moment is inferred from thermionic and contact-potential measurements of the change in work function during adsorption. To obtain surfaces that are both clean and well-defined, single-crystal specimens are employed together with ultrahigh vacuum techniques. During the past year, we have studied the adsorption of various alkali metals, halogens, and oxygen on the (100) face of tungsten and the (110) face of tantalum. This work will be extended during the coming year, and we also plan to construct an apparatus for detecting surface impurities by Auger electron spectroscopy.

2. Oxidation of Metals at High Temperature and Low Pressure

Recently, we have formulated a quasi-thermodynamic approach to heterogeneous chemical reactions occurring at gas-solid interfaces. This approach has been applied to the reaction of gaseous O_2 with various solids (W, Mo, and C) at high temperature and low pressure where the reaction products (oxides) are volatile. Considering the simplicity of the approach, the calculated evaporation rates of the various volatile products agree surprisingly well with existing mass-spectrometric data on these reactions, especially when we account for the fact that not all of the impinging molecules are equilibrated to the surface. Both steady-state and transient ("flash desorption") reactions have been considered, and we now plan to extend the treatment to other gas-solid systems.

3. Catalytic Reactions at Gas-Solid Interfaces

The above-mentioned quasi-thermodynamic approach to heterogeneous reactions is also being applied to catalytic reactions, especially those relevant to the control of air pollution. At present, we are considering reactions involving NO, CO, CO_2, N_2, and O_2. The results of these computations will be compared with existing data obtained with various catalytic materials. In the future, we plan to utilize molecular-beam and mass-spectrometric techniques to determine the kinetics of these reactions for several different single-crystal catalysts.

4. Scattering of Gas Atoms and Molecules from Solid Surfaces

During the past year, we have completed the construction and development of a modulated molecular-beam apparatus designed for investigating the collisions of gas atoms and molecules with solid surfaces. The principal goal is to determine the dependence of energy and momentum transfer on the properties of the gas and the solid, and on the structure and composition of the surface. Data have been obtained for the scattering of Ar atoms from Si(111), Ta(110), and W(110), and for the scattering of Ne from W(110). The W(110) surface was intentionally contaminated with O_2 and with CO for the purpose of determining the sensitivity of the scattering pattern to the degree of surface contamination. These results illustrate the potential usefulness of low-energy molecular scattering (LEMS) as a technique for studying both the properties of solid surfaces and the dynamics of gas-solid collisions. Our current objective is to obtain similar data for a variety of beam gases, contaminants, and solid surfaces.

5. Absorption, Permeation, and Desorption Processes for
    Gases Dissolved in Metals

Recently, we have developed a theoretical analysis of the permeation of gases through solids which includes the possibility that the rate is limited by surface processes (for example, adsorption and desorption), as well as by diffusion. The results provide a possible explanation for a wide variety of permeation data that cannot be explained by the diffusion process alone. The analysis is now being extended to transient desorption processes in which the temperature of the solid decreases so rapidly that the gas within the solid may not have sufficient time to escape, thereby resulting in supersaturation. We also plan to construct an experimental apparatus for measuring the spatial and speed distributions of H_2 desorbing from various metals; these data should lead to a better understanding of the process of "activated adsorption."

6. Electrode Processes in Electrical Discharges

During the past year, we have conducted experimental and analytical studies of the interaction of arcs or sparks with metallic electrodes, especially for those conditions encountered in electrical discharge machining. The principal objective is to determine the mechanism responsible for the erosion of material from the electrode surfaces. By gaining a clearer understanding of the erosion mechanism, we hope to be able to devise methods for increasing the present levels of tool life and cutting speed of electric discharge machining.

R. E. Stickney

A. QUASI-THERMODYNAMIC ANALYSIS OF THE REACTION OF A GAS WITH A SOLID TO FORM VOLATILE PRODUCTS: FLASH DESORPTION STUDY OF THE OXIDATION OF TUNGSTEN

1. Introduction

In a recent report[1] we described a quasi-thermodynamic treatment of the chemical reaction of gaseous oxygen with solid tungsten under steady-state conditions at low pressure and high temperature. Since the computed rates of evaporation of volatile products were found to agree satisfactorily with existing experimental data, we concluded that, although the treatment is based on an oversimplified model, it may be useful as an approximate description of some gas-solid reactions occurring at steady-state conditions. The objective of this report is to determine if the treatment may be modified so that it is also useful in describing gas-solid reactions that occur under transient conditions such as those encountered in experiments based on the flash desorption technique.

Our primary reason for considering the transient case is that the flash desorption technique has been employed recently by Ptushinskii and Chuikov[2] and by McCarroll[3] to obtain detailed data on the reaction of oxygen with tungsten. Since we shall be referring frequently to the data of Ptushinskii and Chuikov, it is advantageous to summarize the essential features of their experiment. A polycrystalline tungsten ribbon mounted on a pair of electrical leads was placed inside a vacuum chamber that was generally maintained at an oxygen pressure of $\sim 1 \times 10^{-7}$ Torr. The tungsten temperature, T, was controlled by passing an electrical current through the ribbon, and, as illustrated in Fig. XV-1, this allowed the ribbon to be heated ("flashed") from 300°K to 2500°K in ~ 0.2 sec, thereby causing the species adsorbed on the tungsten surface to desorb. A mass spectrometer was positioned immediately in front of the ribbon so that a portion of the species desorbing from the surface passed directly into the ionizer of the mass spectrometer without colliding with solid surfaces. The normal procedure was to flash the ribbon only after it had been held at a specific temperature, T_{ad}, sufficiently long to ensure that the adsorption of oxygen had reached a steady-state value. The data shown in Fig. XV-1 correspond to $T_{ad} = 300°K$, and we see that although atomic oxygen is the predominant species (especially when T rises above 2000°K), the desorption of oxides is significant in the early portion of the flash where the temperature is below 2000°K.

The principal question that we wish to consider is: Can the flash desorption data of Ptushinskii and Chuikov (e.g., Fig. XV-1) be explained by assuming that the transient reaction is a quasi-static process (i.e., a process in which the adsorbate passes through a continuous series of equilibrium states)?
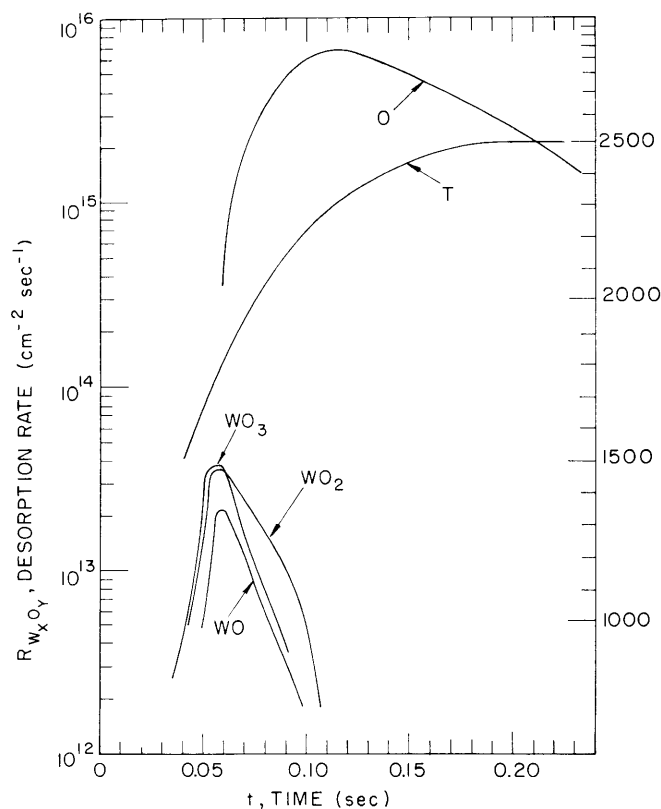
Fig. XV-1. Experimental flash-desorption curves for the reaction of oxygen with a polycrystalline tungsten surface (Ptushinskii and Chuikov[2]). The mass spectrometric signals for the various species have been converted to an absolute scale of desorption rates by the approximate method described in Batty and Stickney.[5]

2. Theoretical Analysis

The present treatment does not require any assumptions concerning which species exist in the adsorbate phase. Therefore, we shall use the symbol [O] to denote the <u>total</u> number of oxygen atoms per cm^2 of the tungsten surface, regardless of whether these atoms actually exist as O, O_2, WO, WO_2, etc. Conservation of oxygen requires that $d[O]/dt$ be equal to the difference between the over-all adsorption and desorption rates for oxygen, and, since the adsorption rate is negligible during the flash desorption process of Ptushinskii and Chuikov, we have

$$\sum y R_{W_x O_y} = -\frac{d[O]}{dt},$$ (1)

where $R_{W_x O_y}$ is the instantaneous value of the desorption rate of species $W_x O_y$. If we

assume that the flash desorption process is quasi-static, then the desorption rates of the various species are related through their equilibrium constants, which may be expressed as[4]

$$K_{W_xO_y} = (2\pi kT)^{1/2}(1-y/2)\left(\frac{M_{W_xO_y}}{M_{O_2}^{y/2}}\right)^{1/2}\frac{R_{W_xO_y}}{R_{O_2}^{y/2}},$$ (2)

where T is the instantaneous temperature, $M_{W_xO_y}$ is the molecular weight of species W_xO_y, and $K_{W_xO_y}$ represents the equilibrium constant for the general reaction

$$xW(s) + \frac{y}{2}O_2(g) \rightleftharpoons W_xO_y(g).$$ (3)

We shall use the "adjusted" values of $K_{W_xO_y}$ defined elsewhere.[5]

Since Eq. 2 provides $r - 1$ equations in terms of r unknown desorption rates (r = number of species), we must have one more equation in order to obtain a solution. In the following calculations this additional equation will be the graphical representation of the experimental results for R_O vs T shown in Fig. XV-1. The procedure is as follows.

1. Choose a value of T and then go to Fig. XV-1 to determine the corresponding value of R_O.

2. With these values of R_O and T, calculate R_{O_2} by means of Eq. 2 for the case $x = 0$, $y = 1$ (that is, $W_xO_y = O$).

3. Use these values of R_{O_2} and T in Eq. 2 to calculate $R_{W_xO_y}$ for each of the major tungsten oxide species.

4. Repeat steps 1 through 3 for various values of T, thereby obtaining a graph of $R_{W_xO_y}$ vs T (or $R_{W_xO_y}$ vs t using the T vs t relation shown in Fig. XV-1).

3. Comparison of Theoretical and Experimental Results

Results obtained by this procedure are presented in Figs. XV-2 and XV-3. To simplify the comparison of Fig. XV-2 with the experimental results in Fig. XV-1, we have omitted from Fig. XV-2 the results for those oxide species that do not appear in Fig. XV-1. Although our computational procedure forces the curves for O in Figs. XV-1 and XV-2 to be identical, it does not force the curves for the other species to agree. In fact, agreement of the curves for a particular species would indicate that the desorption rate for that species equals the "equilibrium" (or quasi-static) value
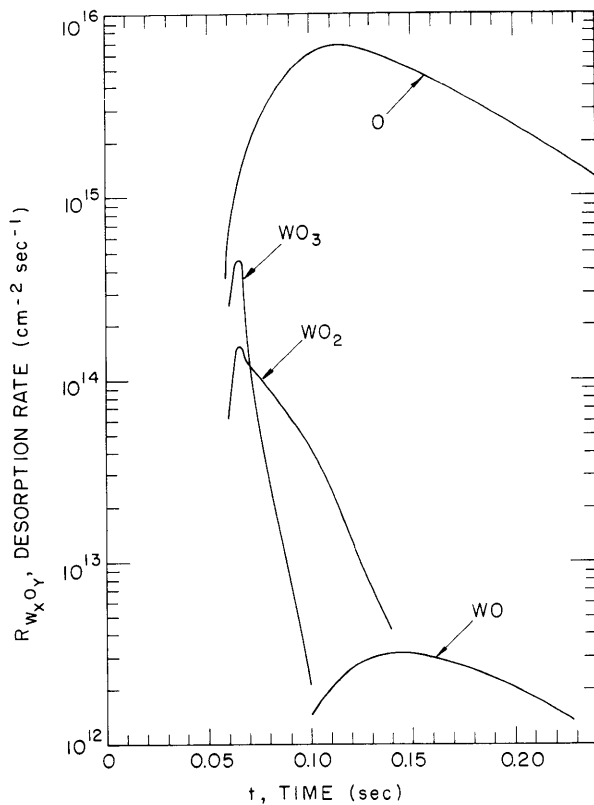
Fig. XV-2.

Theoretical flash-desorption curves for the reaction of oxygen with a tungsten surface. Note: for convenience of comparison with Fig. XV-1, the curves for those species not appearing in Fig. XV-1 have been omitted. (See Fig. XV-3.)
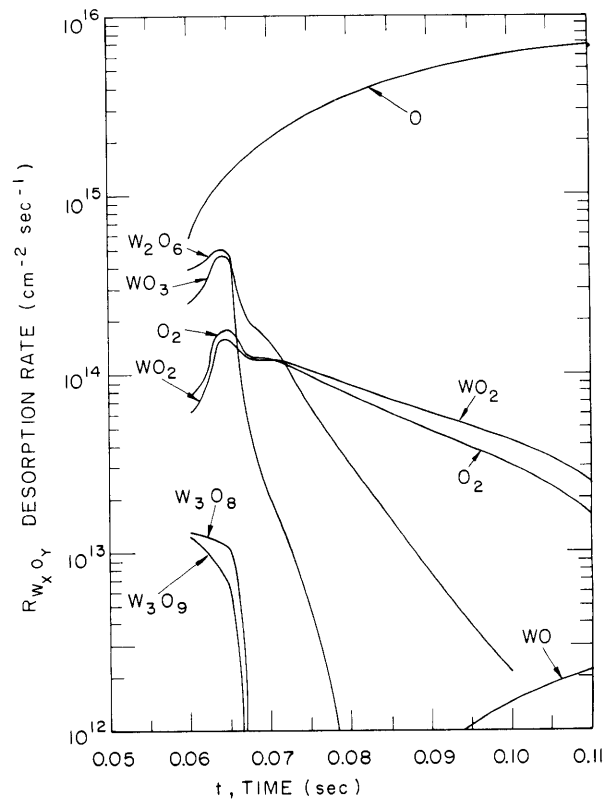
Fig. XV-3.

Theoretical flash-desorption curves for the reaction of oxygen with a tungsten surface. (Conditions are identical to those for Fig. XV-2, but included here are the results for all of the major species, and the time scale has been enlarged for clarity.)

corresponding to the instantaneous values of R_O and T. Notice that the agreement for WO_2 and WO_3 is reasonably good in view of the limited accuracy of both the experimental and theoretical results. (This question of accuracy is considered in detail elsewhere.[5]) The lack of agreement for WO is not surprising because the experimental curve is suspected[2] to be the result of electron-impact induced dissociation of WO_2 and WO_3.

The theoretical results for all of the major species are shown in Fig. XV-3 on an enlarged time scale for clarity. Although the magnitudes of the results for W_2O_6 and O_2 suggest that these species should have been detectable, their absence in the experimental results (Fig. XV-1) may be due to one or more of the following causes: (i) the O_2 signal was obscured by wall effects,[2] (ii) the equilibrium constant used to calculate the W_2O_6 rate may be erroneous, (iii) the T vs t relation shown in Fig. XV-1 may not be completely accurate in the range 1500-2000°K, thereby causing $R_{W_2O_6}$ to be too

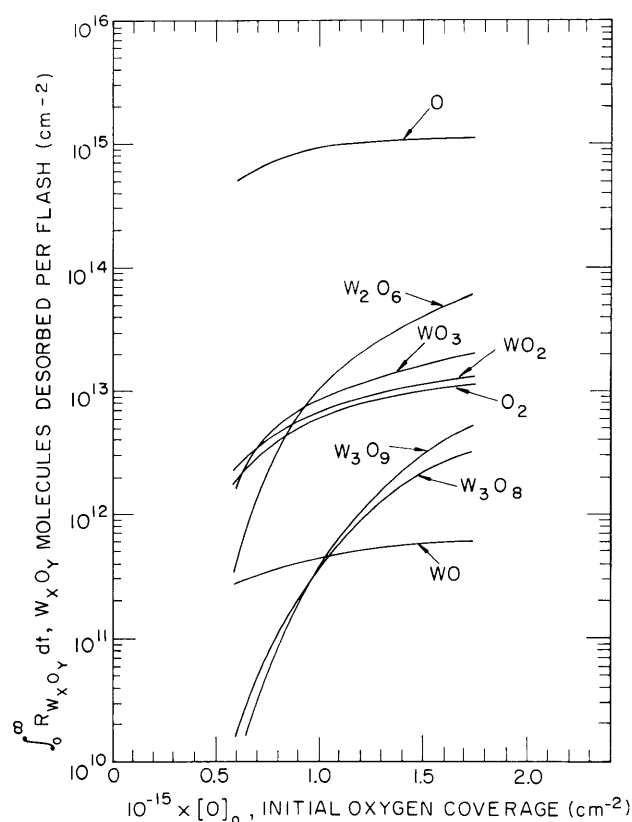Fig. XV-4. Theoretical dependence of the amount of each species desorbed per cm^2 per flash on the total amount of oxygen initially adsorbed on the tungsten surface before the flash.

large,[6] and (iv) the conversion factor used in converting the raw experimental data to the absolute scale of desorption rate shown in Fig. XV-1 may be slightly high. The importance of point (iv) is illustrated in Fig. XV-4 which was computed in the following manner. If we assume that the effect of the erroneous conversion factor may be corrected by multiplying the ordinate in Fig. XV-1 by a constant factor, a, then the corrected value of R_O is a times that shown in Fig. XV-4. This corrected value of R_O is used to calculate new results to replace those in Figs. XV-2 and XV-3. With these results we calculate both the number of molecules of species $W_x O_y$ desorbed per cm^2 per flash,

$$\int_0^\infty R_{W_x O_y} \, dt \tag{4}$$

and the total amount of oxygen desorbed per cm^2 per flash,

$$[O]_o = \sum_x \sum_y \int_0^\infty yR_{W_xO_y} \, dt \qquad (5)$$

which is numerically equal to $[O]_o$, the oxygen coverage initially on the surface before
the flash. (The oxygen coverage, denoted by $[O]$, is defined as the total number of
O atoms adsorbed per cm^2 of surface area, regardless of whether these atoms actually
exist in the adsorbate as O, O_2, W_xO_y, or a mixture of these species.) Each value of
a results in different values of $\int_0^\infty R_{W_xO_y} \, dt$ and $[O]_o$, and the results given in Fig. XV-4
were obtained by repeating the calculations for a ranging from 0.7 to 1.6. Notice that
the amount of W_2O_6 relative to either WO_2 or WO_3 decreases sharply as $[O]_o$ decreases
(that is, as a decreases). Since $[O]_o \approx 0.8 \times 10^{15} \; cm^{-2}$ for the results shown in
Figs. XV-2 and XV-3, we conclude from Fig. XV-4 that the relative amount of W_2O_6
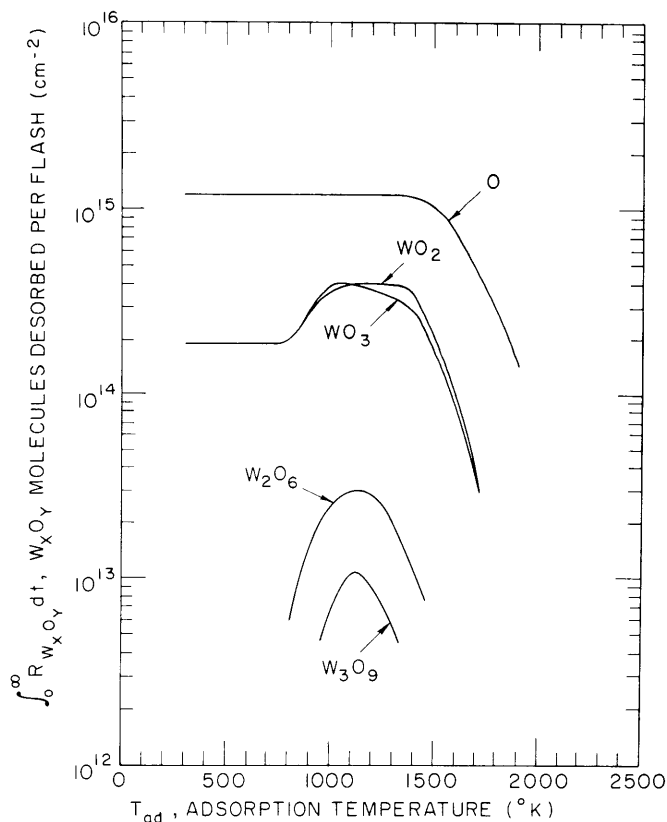is very sensitive to a small error in the conversion factor used in constructing
Fig. XV-1.

Fig. XV-5. Experimental results of the effect of adsorption tempera-
ture on the amounts of the various species desorbed per
cm^2 per flash. (Replotted from Ptushinskii and Chuikov.[2])

Ptushinskii and Chuikov[2] also performed a series of experiments in which they varied T_{ad}, the temperature at which the tungsten ribbon was held during adsorption of oxygen before the flash. These data (Fig. XV-5) show that $\int_0^\infty R_{W_xO_y} dt$, the amount of species W_xO_y desorbed per cm^2 per flash, depends on T_{ad} in a rather complicated manner. Although the amounts of the various species desorbed are seen to be independent of T_{ad} in the range $300-\sim750°K$, the amounts of all species other than O increase markedly if the adsorption process is performed at temperatures in the range $750°K \lesssim T_{ad} \lesssim 1150°K$, thereby indicating an increase in $[O]_o$, the total amount of oxygen adsorbed on the surface before the flash. This increase in $[O]_o$ with T_{ad} has also been reported by other investigators[7] using different experimental techniques, and the common explanation is that the adsorption of oxygen at high coverages is a thermally activated process. At too high temperature, however, the adsorbate becomes thermally unstable, and causes $[O]_o$ to decrease with increasing T_{ad}, as indicated in Fig. XV-5 by the fact that the amounts fall off for $T_{ad} \gtrsim 1250°K$.
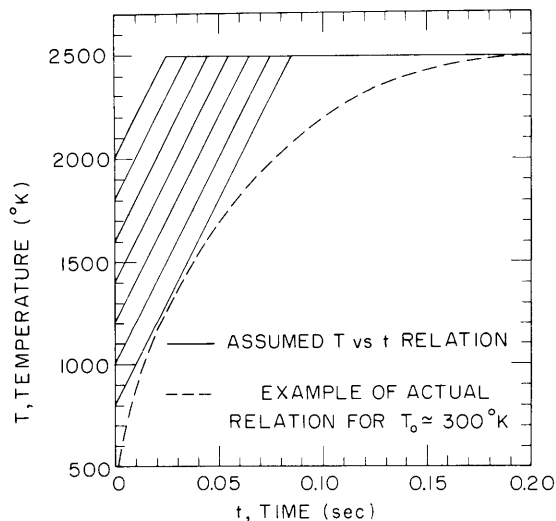

Fig. XV-6.

Assumed dependence of temperature on time for flash-desorption processes originating at different initial values of T_{ad}, the adsorption temperature immediately preceding the flash. For comparison, the experimental curve from Fig. XV-1 is included.
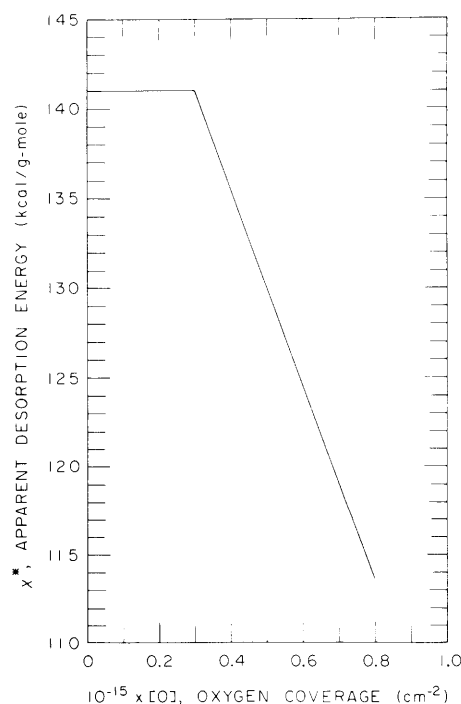

Fig. XV-7.

Assumed dependence of the apparent desorption energy, χ^*, on oxygen coverage, $[O]$. (This relation has been estimated from experimental data[2] by the procedure described in Batty and Stickney.[5])
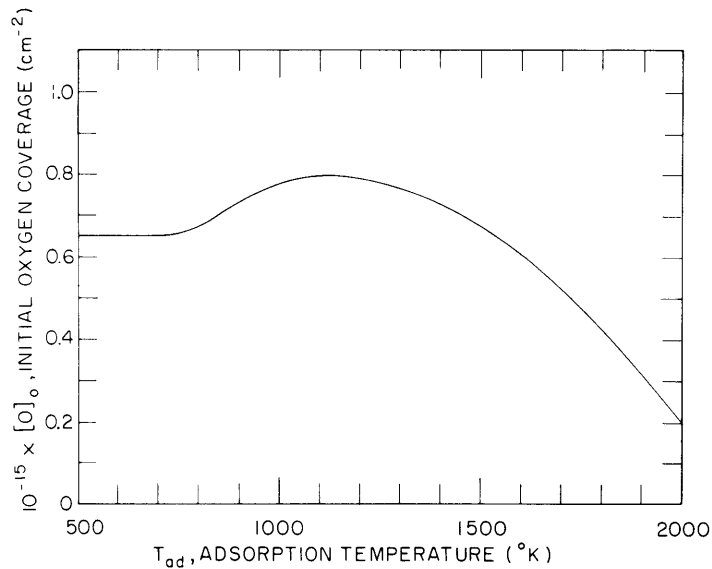
Fig. XV-8.   Assumed relation for the total amount of oxygen
adsorbed at various temperatures.

If we accept the argument that $[O]_o$ increases with T_{ad} in the range 700-1150°K, then the theoretical results given in Fig. XV-4 provide a possible qualitative explanation for the experimental observation (Fig. XV-5) that the amount of oxygen desorbed as oxides increases in this range, whereas the amount desorbed as O remains essentially unchanged. As may be seen in Fig. XV-4, an increase in $[O]_o$ causes a greater increase in the oxides than in atomic oxygen, especially for $[O]_o > 1 \times 10^{15}$. The results in Fig. XV-4 are not a suitable basis for making a closer comparison of experimental and theoretical results because they were calculated by using the T vs t relation shown in Fig. XV-1, which is valid only for T_{ad} = 300°K. Since Ptushinskii and Chuikov[2] do not report the T vs t relations for flashes starting at different values of T_{ad}, we shall base the following computations on the oversimplified linear relations shown in Fig. XV-6. Similarly, the lack of experimental data on R_O vs t for different T_{ad} will be compensated for by assuming that R_O may be represented by the expression[8]

$$R_O = kT/h[O] \exp(-\chi^*/kT),\qquad\qquad(6)$$

where k and h are Boltzmann's and Planck's constants, respectively, and χ^* is the apparent desorption energy, which is assumed to vary with coverage in the manner shown in Fig. XV-7. (This approximate relation for χ^* vs [O] was estimated[5] by fitting Eq. 6 to the experimental data for R_O vs t given in Fig. XV-1.) The final assumption is that the dependence of coverage on adsorption temperature may be approximated by the curve shown in Fig. XV-8. Using these assumptions, we have calculated the curves
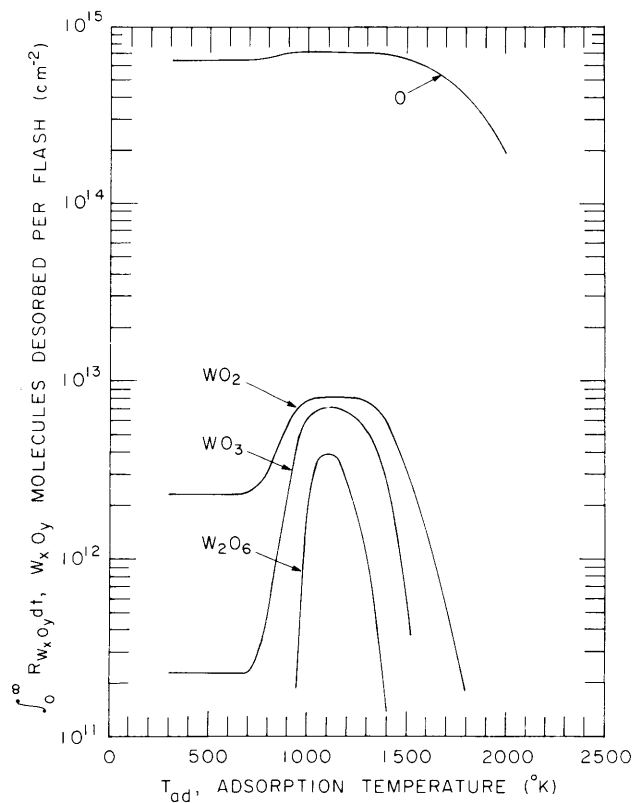
Fig. XV-9. Theoretical prediction of the effect of adsorption tempera-
ture on the amount of the various species desorbed per
cm^2 per flash.

shown in Fig. XV-9, which are qualitatively similar to the experimental curves in Fig. XV-5. The agreement could be improved by slight changes in the assumed relations (Figs. XV-6, XV-7, and XV-8), but quantitative agreement should not be expected, in view of the numerous oversimplifications and the limited accuracy of the data.

4. Concluding Remarks

The development of an atomistic theoretical model of the kinetics of the oxygen-tungsten reaction is a formidable task, and at present those concerned with this problem do not even agree on some of the most basic mechanisms. For example, McCarroll's view[3] is that the oxide molecules that desorb from the surface are formed at low temperature before the flash, whereas Ptushinskii and Chuikov[2] question this view and suggest that the oxides may have formed during the flash. Schissel and Trulson[9] have described a kinetic model in which two states of adsorption are assumed. The quasi-thermodynamic approach presented here circumvents the problem of formulating an atomistic kinetic model of the reactions among the adsorbate species, and results are

obtained without making any assumptions about whether the adsorbate consists of atoms, molecules, radicals, or complexes.

Since the results of the present analysis agree, at least qualitatively, with both the steady-state[1] and flash-desorption experimental data, we have reasonable support for the idea that the desorption process of the oxygen-tungsten reaction does not deviate radically from being a quasi-static process. That is, both the rates of the reactions occurring within the adsorbate phase and the rates of desorption of the various species are sufficiently rapid that the desorbing species remain in chemical equilibrium with one another even for transient conditions in which T and [O] vary with time.

A detailed discussion of this work is being written,[5] and similar computations are being performed for other gas-solid systems.

J. C. Batty, R. E. Stickney

References and Footnotes

1. J. C. Batty and R. E. Stickney, Quarterly Progress Report No. 89, Research Laboratory of Electronics, M.I.T., April 15, 1968, pp. 57-64.

2. Yu. G. Ptushinskii and B. A. Chuikov, Surface Sci. 6, 42 (1967); 7, 90 and 507 (1967).

3. B. McCarroll, J. Chem. Phys. 46, 863 (1967); Surface Sci. 7, 499 (1967).

4. See Eqs. (2) and (7) in J. C. Batty and R. E. Stickney, Quarterly Progress Report No. 89, op. cit.

5. J. C. Batty and R. E. Stickney (unpublished paper to be submitted to the Journal of Chemical Physics).

6. A slight change in the T vs t relation causes a substantial change in the relative magnitudes of the computed curves in Figs. XV-2 and XV-3 because the instantaneous value of oxygen coverage at arbitrary time t and temperature T depends strongly upon the preceding temperature-time history.

7. J. H. Singleton, J. Chem. Phys. 47, 73 (1967); Ya. P. Zingerman and V. A. Ishchuk, Soviet Phys. — Solid State 6, 904 (1964); 7, 173 (1965).

8. For a discussion of this expression for R_O, see D. O. Hayward and B. M. W. Trapnell, Chemisorption (Butterworths, London, 1964), see Chap. 4.

9. P. O. Schissel and O. C. Trulson, J. Chem. Phys. 43, 737 (1965).

B. CONTACT-POTENTIAL MEASUREMENTS OF THE ADSORPTION OF I_2, Br_2, AND Cl_2 ON A (100) TUNGSTEN CRYSTAL

1. Introduction

The adsorption of alkali metals on metallic surfaces has recently received considerable attention because (i) alkalis are being employed in thermionic energy conversion, ion propulsion, and MHD devices, and (ii) the monovalent nature of the alkalis makes them more amenable to theoretical analysis than for polyvalent species. Various

theoretical treatments have been proposed,[1,2] but it is impossible to judge their validity solely by comparison with experimental data for alkali adsorption because all of these treatments were designed to agree with the alkali data. A more rigorous test of the theoretical treatments would be to compare their predictions with experimental data for other adsorbate species. The halogen gases are one of the most logical choices of adsorbates for this test because they are the electronegative analog of the alkali metals. This point, together with the fact that halogens are being considered as possible additives to thermionic converters, have motivated the present experimental investigation of the adsorption of I_2, Br_2, and Cl_2 on W(100).

2. Experimental Apparatus

Except for the halogen gas sources and the W(100) crystal, the apparatus was identical to that described previously.[3] The (100) oriented tungsten single crystal was a disc, 6 mm in diameter, mounted at one end of a tungsten tube. The crystal could be heated to ~1100°K by radiation from a tungsten filament located inside the mounting tube, and higher temperatures were attained by electron-bombardment heating. Crystal-temperature measurements were made by means of a W 5% Re-W 25% Re thermocouple welded to the tungsten tube. Contact-potential measurements were based on the electron-beam retarding potential technique described previously.[3,4]

The halogen pressures were measured with an ionization gauge, and, since accurate gauge sensitivity values were not available for halogens, we used the direct reading (equivalent N_2 pressure) as an estimate of the pressure throughout the present study. A monopole partial pressure analyzer was used to determine the relative composition of the chamber gas.

The halogen sources were 1-liter flasks with break-off seals mounted on a common manifold that was joined to the main system by a bakeable variable-leak valve. After opening the break-off seal, but before admission of the given halogen into the system, the halogen flask was cooled and pumped for several hours to remove impurity gases. The I_2 and Br_2 were pumped at two different temperatures, ~77°K and ~250°K, whereas Cl_2 was pumped only at 77°K. Between pumping runs, the halogen was allowed to warm up and was then recooled and distilled back to the bottom of the source flask to allow any gases trapped in the solid or liquid halogen to escape. In addition to these precautions, the vacuum chamber and glass manifold of the halogen-handling system were always baked to remove water vapor before the admission of the halogen. Despite these precautions, admission of I_2, Br_2, or Cl_2 into the system always produced an H_2 peak in the mass spectrum in addition to molecular and atomic halogen peaks. At all except the highest halogen pressures, the H_2 fraction of the total pressure was nearly constant at ~4% for all of the halogens. At pressures in the 10^{-6}-10^{-5} Torr range the H_2 fraction decreased to 1-2%. Although the origin of the H_2 is uncertain, it does not appear that

it is present as an impurity in the halogen flasks, since no H_2 peak was detected when the flask was cooled to ~77°K with the valve to the system fully opened. This suggests that H_2 is formed by an interaction of the halogen with the stainless-steel walls of the vacuum chamber, possibly an interaction with water vapor not driven off the walls by bakeout. The important question is what effect the relatively large H_2 background might have on our halogen adsorption studies. As will be seen, the results of a few studies with very high (~25% of total pressure) H_2 backgrounds indicate a negligible effect of the H_2 background upon our halogen studies, a result which may not be too surprising, since it appears that halogens displace adsorbed hydrogen.

3. Experimental Results

a. I_2 on W(100)

The results for I_2 adsorption on W(100) at ~300°K are shown in Fig. XV-10. The solid curve is an average of eleven runs made over a period of several weeks. The maximum spread of the data, in terms of both N and $\Delta\phi$, is indicated by bars at various positions. Also, two runs are shown which fall outside the spread of N but within the $\Delta\phi$ spread both at the minimum and at the high-coverage plateau. This last agreement, plus the similarity in shape to the average curve, suggests that the deviation of these curves is caused primarily by imprecise pressure measurements.
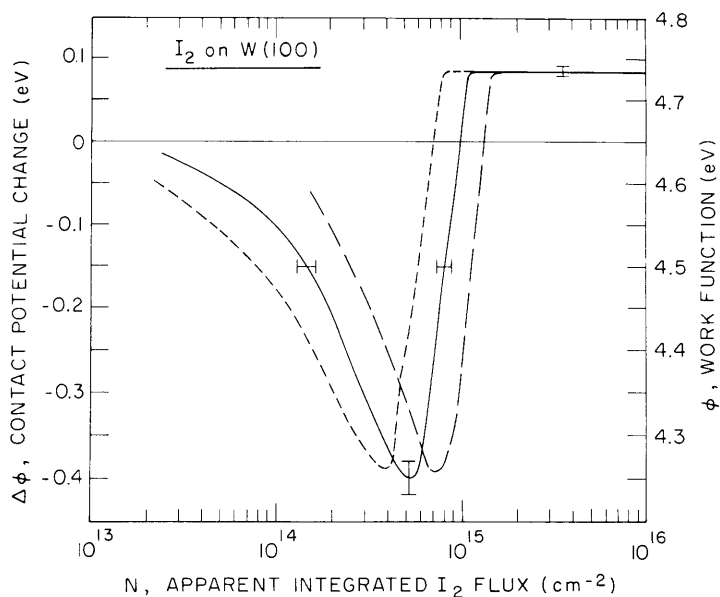

Fig. XV-10. Contact-potential data for the adsorption of I_2 on W(100) at $T_s \approx$ 300°K and pressures in the range 5×10^{-9}–1×10^{-6} Torr.

The data in Fig. XV-10 were obtained for apparent I_2 pressures ranging from 5×10^{-9} to 1×10^{-6} Torr so that we could determine whether the value of ϕ_f, the final work function, is pressure-dependent. (The "final" work function, ϕ_f, denotes the value of ϕ attained in the high-coverage limit.) A systematic dependence of ϕ_f on pressure was not observed, and this constitutes indirect evidence that the final coverage is independent of pressure in the present range.

The unusual feature of Fig. XV-10 is that the work function <u>decreases</u> during the initial stage of adsorption. A maximum decrease of 0.4 ± 0.02 eV below the bare sur- face value occurs when N reaches $\sim 5 \times 10^{14}$ cm^{-2}. With further increase of N, ϕ increases abruptly and finally attains a limiting value of 0.088 ± 0.01 eV <u>above</u> the bare surface value when N reaches $\sim 1 \times 10^{15}$ cm^{-2}.

To determine the possible influence of H_2 adsorption on the I_2 data, four runs were made after the system had been exposed to a high pressure of I_2. The valve was closed and contact-potential measurements were made during the transient stage in which the residual I_2 and H_2 were slowly pumped away. The pump apparently had a faster pumping speed for I_2 than for H_2, for during the transient stage the apparent H_2 partial pressure became ~ 20-25% of the apparent total pressure. In all of these runs the minimum work functions fell within the data spread indicated in Fig. XV-10, while the final work func- tions, ϕ_f, fell no more than 0.012 eV above the maximum spread. These results indi- cate that the level of H_2 existing in the normal I_2 adsorption runs was too low to have a significant effect on the data.

Qualitative studies of the desorption of iodine from W(100) were performed in the following manner. First, the surface was exposed to I_2 until the high-coverage limit of $\phi = \phi_f$ was achieved. Next, the I_2 was pumped out, and the crystal was heated to tem- perature T for 3 min. The crystal was then allowed to cool for ~ 3 min so as to return to $\sim 300°$K, at which time the contact potential was measured. This cycle was repeated for $\sim 50°$ increments of T up to $\sim 1100°$K, the highest temperature attainable by radiant heating alone. The results indicated that desorption began at temperatures as low as $450°$K, and at $\sim 770°$K the work function corresponded closely to the minimum value in Fig. XV-10. The work function remained essentially constant at this value for $\sim 770°$K$<$ T $<$ $900°$K. Heating cycles for $900°$K $<$ T $<$ $1100°$K caused a progressive change in ϕ toward the bare surface value, but desorption did not appear to be complete even at $1100°$K. Heating to $1500°$K was sufficient for complete desorption, as indicated by the fact that ϕ was restored to the bare surface value. These results agree with the flash desorption data of McCarroll,[5] thereby indicating that at high coverage molecular iodine desorbs from a molecular adsorption state at $\sim 500°$K, and at low coverage atoms desorb from an atomic state at $\sim 1500°$K. The fact that a drastic change in the apparent binding energy occurs very near the work-function minimum in our data indicates that the initial decrease in ϕ is associated with the atomic adsorption state, whereas the increase in

ϕ at higher coverages is associated with the molecular state. Since accurate values for the sticking coefficient of I_2 on W(100) and the ion gauge correction for I_2 are not available, we cannot convert the apparent integrated flux scale in Fig. XV-10 to an accurate measure of coverage. It is interesting to note, however, that the work-function minimum in Fig. XV-10 occurs at an apparent integrated <u>atomic</u> flux of $2N \approx 1.05 \times 10^{15}$ cm^{-2}, which is a reasonable order of magnitude for an atomic monolayer. The density of W atoms on a W(100) surface is $\sim 1 \times 10^{15}$ cm^{-2}.

During the lower coverage, high-temperature portion of the desorption runs, results were obtained which indicated a moderate temperature coefficient of work function for I on W(100). Because of the massiveness of the W crystal and support, ~ 3 min was required to cool to $\sim 300°$K following heating during desorption runs. During higher temperature ($\sim 1000°$K) desorption runs, contact-potential measurements were made both 15-30 sec and 3-4 min after heating power was turned off. Since the time dependence of the temperature following power shutoff was known, it was then possible to estimate the temperature coefficient from the difference between the two contact-potential measurements. In the low-coverage region we obtained $\partial\phi/\partial T \approx +1 \times 10^{-4}$ eV/$°$K.

b. Br$_2$ on W(100)

Immediately after changing from I_2 to Br$_2$ we observed unusually high residual partial pressures corresponding to iodine plus some iodides, most likely because Br$_2$ displaces these species from the chamber walls. This problem was partially overcome by exposing the system to Br$_2$ at $\sim 1 \times 10^{-6}$ Torr for several days. Following this treatment, the apparent I_2 pressure was <1% of the apparent Br$_2$ pressure for total pressures in the high 10^{-7} Torr range and above, and it was <5% in the range below $\sim 1 \times 10^{-7}$ Torr. Most of the Br$_2$ runs were conducted under these conditions, but subsequently the chamber was baked and the I_2 signal returned even stronger than before, reaching a level of $\sim 50\%$ of the apparent total pressure. Results for this nearly equal mixture of Br$_2$ and I_2 will be presented.

Results for the adsorption of Br$_2$ on W(100) at $300°$K are presented in Figs. XV-11 and XV-12. In Fig. XV-11 results are shown for the lower pressure, lower total flux runs, with the dashed curve representing an average of three runs made at apparent Br$_2$ pressures ranging from 5×10^{-9} Torr to 1×10^{-8} Torr. The spread of these data was negligible. The solid curve represents an average of five other runs made at pressures ranging from 7×10^{-9} Torr to 1×10^{-7} Torr, and the maximum data spread is indicated by bars. As in the case of I_2, it appears that the major difference between the two sets of data arises from erratic pressure measurements, since the two curves could be made to agree within the limits of measurements simply by multiplying the pressure readings for one curve by a constant.

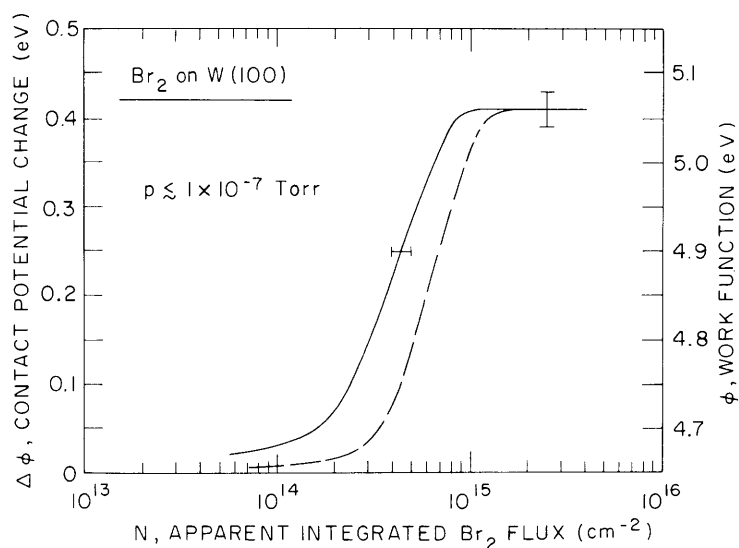The data in Fig. XV-11 indicate that ϕ increases monotonically with Br$_2$ coverage,
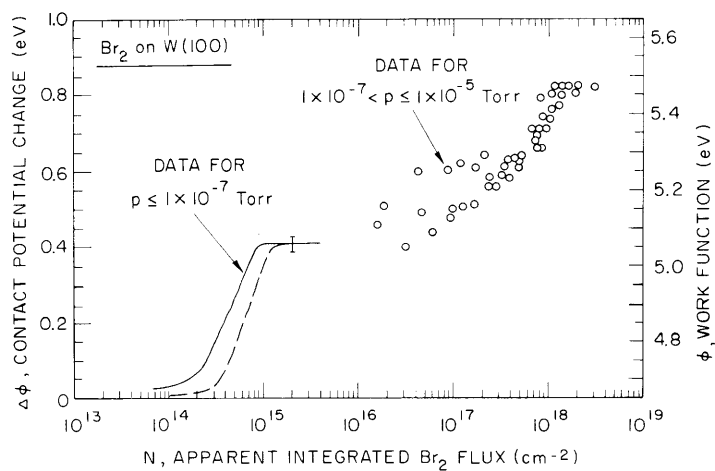
Fig. XV-11. Contact-potential data for the adsorption of Br_2 on W(100) at $T_s \approx$ 300°K and pressures in the range 5×10^{-9}–1×10^{-6} Torr.

Fig. XV-12. Contact-potential data for the adsorption of Br_2 on W(100) at $T_s \approx$ 300°K and pressures in the range 5×10^{-9}–1×10^{-5} Torr.

attaining a maximum increase of 0.41 ± 0.02 eV above the bare surface value at $N \approx$ 1×10^{15} cm^{-2}. At higher Br$_2$ pressures, however, ϕ continued to increase as shown in Fig. XV-12. Although the scatter is large in the intermediate range, the data are sufficient to indicate that Br$_2$ adsorption depends markedly on pressure. For $N \geq 2 \times 10^{18}$ cm^{-2} it appears that ϕ approaches a limiting value ~0.82 eV above the bare surface value. This value was stable even when the Br$_2$ pressure was reduced to ~10^{-9} Torr.

Bromine desorption experiments were conducted in the same manner as described for iodine, and the results indicate that a temperature of ~550°K is sufficient to desorb the molecules responsible for work functions in the range $0.41 \leq \Delta\phi \leq 0.82$ eV. The value $\Delta\phi \approx 0.41$ eV remained essentially constant in the range ~550°K $< T <$ 900°K, thereby indicating negligible desorption. The work function decreased monotonically for 900°K $< T <$ 1100°K, and, as in the case of iodine, a temperature of ~1500°K was sufficient to restore ϕ to the bare surface value. These data indicate that the binding energies of Br and I on W(100) are approximately equal in the low-coverage limit. This result is consistent with flash-desorption measurements by McCarroll[5, 6] which yield binding energies of ~88 kcal and ~80 kcal for Br and I, respectively, on polycrystalline W. McCarroll[6] did not observe a significant low binding energy state for Br$_2$, and this may be the result of lower adsorption pressures and/or the fact that his tungsten ribbon was not an oriented (100) crystal.

The temperature coefficient of the work function of the Br-W system was determined by the same procedure as for I-W. In the lower coverage range we obtained $\partial\phi/\partial T \approx +1 \times 10^{-4}$ eV/°K.

As in the preceding study of I$_2$ adsorption, H$_2$ constituted ~4% of the total pressure after Br$_2$ was admitted to the system. To test the possible effect of H$_2$ on the results, a few runs were made in which the H$_2$ background was increased to ~20% of the total pressure by the same method as described above. These runs were made only for the lower pressure region and, in this case, an apparent final work function ~0.41 eV above the bare surface value was obtained, thereby indicating that the H$_2$ background has a negligible effect on the results.

Figure XV-13 shows the results of the set of 7 runs in which the Br$_2$ displaced I$_2$ from the chamber walls to produce a mixture consisting of ~50% Br$_2$ and ~50% I$_2$. (Note that in calculating the integrated flux for Fig. XV-13, the total pressure was treated as if it consisted entirely of Br$_2$.) These results are qualitatively similar to those obtained for I$_2$ adsorption alone. In the low-coverage region the work function decreases; however, the maximum decrease is 0.14 eV as compared with 0.4 eV for I$_2$ alone. Beyond the minimum, the work function increases until a value 0.1 eV above the bare surface value is obtained, as compared with 0.088 eV obtained for adsorption of I$_2$ alone.
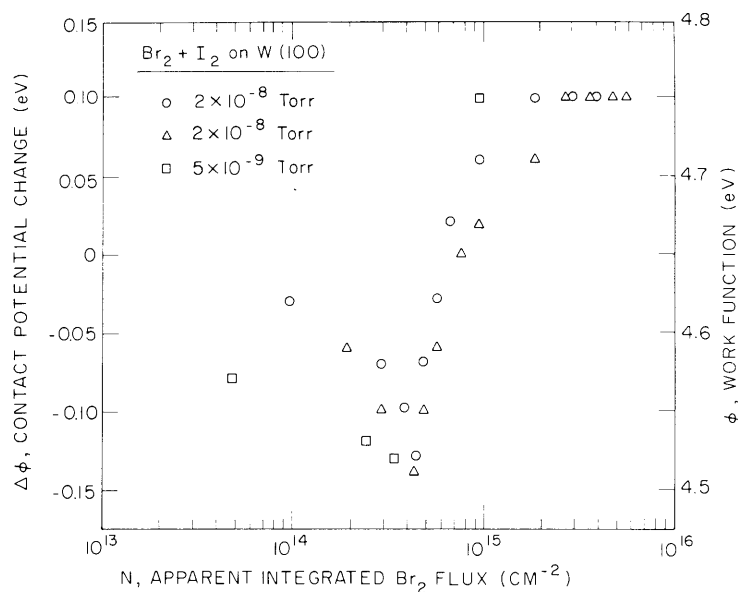
Fig. XV-13. Contact-potential data for the coadsorption of Br_2 and I_2 on W(100) at $T_s \approx 300°K$.

c. Cl_2 on W(100)

The results for Cl_2 adsorption on W(100) are shown in Fig. XV-14 where data from 10 runs for Cl_2 pressures ranging from 1.5×10^{-9} Torr to 4×10^{-6} Torr have been averaged to obtain the solid curve with maximum spread indicated by bars. Although not shown in Fig. XV-14, the high-coverage limit of $\Delta\phi = 0.635$ eV was observed to remain constant for N as large as 3×10^{17} cm^{-2}.
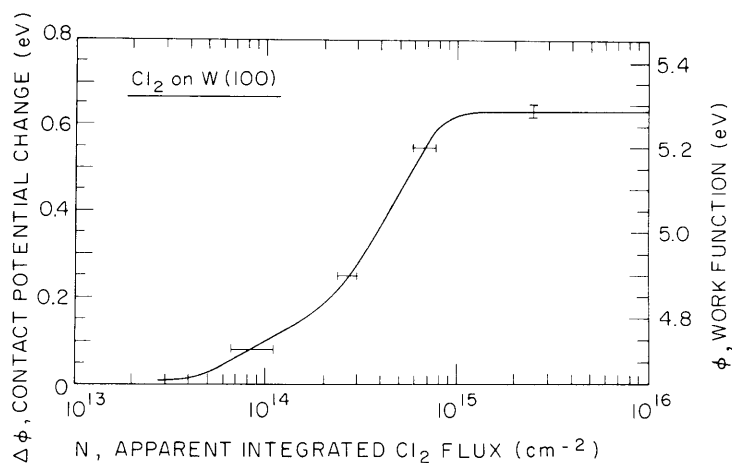

Fig. XV-14. Contact-potential data for the adsorption of Cl_2 on W(100) at $T_s \approx 300°K$ and pressures in the range 1.5×10^{-9}-4×10^{-6} Torr.

The Cl_2 data behave in a much more regular fashion than either the Br_2 or I_2 data, possibly because the behavior of the ionization gauge is less erratic for Cl_2 than for I_2 or Br_2. The work function increases monotonically with coverage toward a limiting value of $\Delta\phi_f = 0.635 \pm 0.015$ eV. This high-coverage limit was independent of pressure throughout the present range, 1.5×10^{-9} Torr to 4×10^{-6} Torr.

The results of desorption tests indicate that significant desorption of chlorine does not occur below ~1000°K. Even after 3 min, each at ~975°K, ~1050°K, and ~1100°K, the work function was still ~0.4 eV above the bare surface value. The temperature coefficient of the work function of the Cl-W system at low coverage was $\partial\phi/\partial T \approx +1 \times 10^{-4}$ eV/°K.

Introduction of Cl_2 into the system did not lead to a large-scale displacement of either bromine or iodine from the chamber walls. There was no indication of a genuine bromine signal in the mass spectrum, and the iodine signal was less than 1% of the total pressure. There was, however, the usual H_2 component comprising ~4% of the total pressure. The possible effect of the H_2 background was studied by the same technique used for both I_2 and Br_2. Just as in the cases of I_2 and Br_2, raising the H_2 pressure to ~20% of the total caused a negligible change in ϕ_f.

4. Summary

One original purpose of this study was to see if work-function changes resulting from halogen adsorption on a W(100) surface could be explained by treating the adsorption as an electronegative analog of alkali-metal adsorption. According to the theoretical treatment of Steiner and Gyftopoulos,[2] the adsorption of halogens on tungsten should cause ϕ to increase, and the magnitude of $\Delta\phi$ at a given coverage should increase with the atomic radii of the halogens, the order being I > Br > Cl. Our experimental results are almost completely contrary to these predictions, both with respect to the relative order and to the sign of $\Delta\phi$ for low iodine coverages. (Over the range for which halogen adsorption is suspected to be predominantly atomic, the maximum values of $\Delta\phi$ are -0.4 eV, +0.41 eV, and +0.635 eV for I, Br, and Cl, respectively.) These results indicate that the adsorption of halogens cannot be explained by a simple extension of theoretical treatments developed for alkali adsorption. The decrease in work function observed for low iodine coverages has also been observed for the adsorption of other electronegative species on tungsten,[3,7] and it is suspected to be the result of rearrangement of the surface atoms and/or penetration of adsorbed atoms into the bulk.

For both iodine and bromine, a low binding state existing at high coverages increased the work function leading to final values 0.088 eV and 0.82 eV, respectively, above the bare surface value. Comparison with existing data[5] indicates that, for iodine at least, this low binding energy state is a molecular state. Over the range of experimental variables used, the adsorption of Cl_2 on W(100) gave no indications of a low binding

energy state. Finally, in the low-coverage region the adsorption of any of the three halogens on W(100) was found to lead to a value of $\partial\phi/\partial T \approx +1 \times 10^{-4}$ eV/°K for the temperature coefficient of the work function.

D. L. Fehrs, R. E. Stickney

References

1. N. S. Rasor and C. Warner, J. Appl. Phys. **35**, 2589 (1964); J. Levine and E. P. Gyftopoulos, Surface Sci. **1**, 171, 225, and 349 (1964); L. D. Schmidt and R. Gomer, J. Chem. Phys. **45**, 1605 (1966); A. J. Bennett and L. M. Falicov, Phys. Rev. **151**, 512 (1966); J. W. Gadzuk, Surface Sci. **6**, 133 (1967); Proceedings of 4th International Materials Symposium on "The Structure and Chemistry of Solid Surfaces" (in press). References to earlier theoretical treatments are given in the paper by Rasor and Warner.

2. D. Steiner and G. P. Gyftopoulos, in Report on 27th Annual Conference on Physical Electronics, M. I. T. , 1967, pp. 160 and 169; also Report on 1967 Thermionic Conversion Specialist Conference (IEEE, 1967), p. 145.

3. D. L. Fehrs and R. E. Stickney, Surface Sci. **8**, 267 (1967).

4. D. L. Fehrs and R. E. Stickney, in Quarterly Progress Report No. 82, Research Laboratory of Electronics, M. I. T. , July 15, 1966, pp. 77-82; No. 84, January 15, 1967, pp. 82-89; No. 88, January 15, 1968, pp. 81-83; No. 91, October 15, 1968, pp. 57-60.

5. B. McCarroll, J. Chem. Phys. **47**, 5077 (1967).

6. B. McCarroll, in Proceedings of the 4th International Materials Symposium on "The Structure and Chemistry of Solid Surfaces" (in press).

7. M. J. Duell, B. J. Davis, and R. L. Moss, Disc. Faraday Soc. **41**, 43 (1966); V. M. Gavrilyuk and V. K. Medvedev, Soviet. Phys. — Solid State **9**, 259 (1967); P. J. Estrup and J. Anderson, in Report on 27th Annual Conference on Physical Electronics (M. I. T. , 1967), p. 47. Also see the references given by D. F. Klemperer, J. Appl. Phys. **33**, 1532 (1962).

C. MOLECULAR-BEAM STUDY OF THE SCATTERING OF NEON ATOMS FROM THE (110) FACE OF TUNGSTEN: THE EFFECT OF ADSORBED O_2 AND CO

1. Introduction

Experimental investigations of the physical and chemical properties of solid surfaces generally are based upon measurements of the interaction of a beam of particles (photons, electrons, neutrons, ions, atoms, or molecules) with the sample. The most popular "probe" particle for surface studies is the electron, partly because the techniques for generating and detecting electron beams are well developed, relatively inexpensive, and compatible with ultrahigh vacuum requirements. Although the techniques for generating and detecting molecular (including atomic) beams are not so far advanced, enough progress has been made recently that it is now feasible to use

molecules as probe particles in certain experiments for which they appear to be the most appropriate choice.[1] Since molecular scattering and low-energy electron diffraction (LEED) provide complementary results, it seems appropriate to refer to the present technique as low-energy molecular scattering (LEMS).

The present LEMS experiment is the first stage of a study of the scattering of gas molecules from single-crystal surfaces, both clean and covered to varying degree with adsorbed molecules. Our long-range objectives may be described in terms of two related questions: What information can LEMS provide on the mechanics of molecular scattering from solid surfaces of specific composition and structure? Which features or properties of surfaces can be studied more directly by LEMS than by other existing techniques? Although the first question has received considerable attention,[2,3] the latter has been almost totally neglected. Very recently, however, Smith and Merrill[4] have shown that in certain cases LEMS is more sensitive than LEED to the condition of a surface.

Since the specific objective of our first experiment is to study scattering from a surface of <u>known</u> composition and structure, tungsten is a convenient choice for the target material because its surface properties and cleaning processes have been studied in more detail than any other metal. We have selected the (110) face of tungsten because there is evidence that it does not become facetted when heated in oxygen.[5] The reasons for choosing O_2 and CO as the adsorbate gases are: (i) detailed LEED data are available on the adsorption and desorption characteristics of these gases on W(110)[5-7]; (ii) since CO is the most common gaseous contaminant of surfaces in ultrahigh vacuum systems, it often complicates the use of other adsorbates; (iii) aside from carbon, O_2 appears to be the most tenacious contaminant of W, and therefore interferes with the use of other adsorbates. Since we wish the "probe" or beam particle to be as simple and as inert as possible, the rare gases are the logical choice. Although the only rare gas utilized in this preliminary experiment is Ne, a similar experiment is now being performed with Ar as the beam gas.

2. Experimental Apparatus

The basic features of the LEMS apparatus are: (i) a nozzle-type molecular-beam source that produces a nearly monoenergetic, high-intensity beam; (ii) a tungsten crystal oriented with the (110) face exposed to the beam; (iii) a rotatable ion gauge for measuring the spatial distribution of the scattered molecules; (iv) preamplifiers and a lock-in detector for processing the signal from the ion gauge; (v) an ultrahigh vacuum chamber having an ultimate pressure in the 10^{-10} Torr range. All of these features, other than the tungsten crystal, have been described previously.[8] The crystal, which is mounted in the manner described by Lee,[9] is a high-purity tungsten (110) single crystal, 6 mm in diameter and 1 mm thick. Although the crystal surface was optically

smooth initially, it degraded early in the experiment to a thermally facetted surface as a result of prolonged heating above 2200°K in vacuum. The crystal is heated by electron bombardment from behind, and its temperature is determined by a W 5% Re-W 25% Re thermocouple.[9]

Flasks of research grade O_2 and CO are connected to the system through a variable-leak valve. This arrangement enables us to expose the crystal to controlled pressures of O_2 or CO.

3. Experimental Results

a. Scattering of Ne from W(110) for Both Clean and Unintentionally Contaminated Surface Conditions

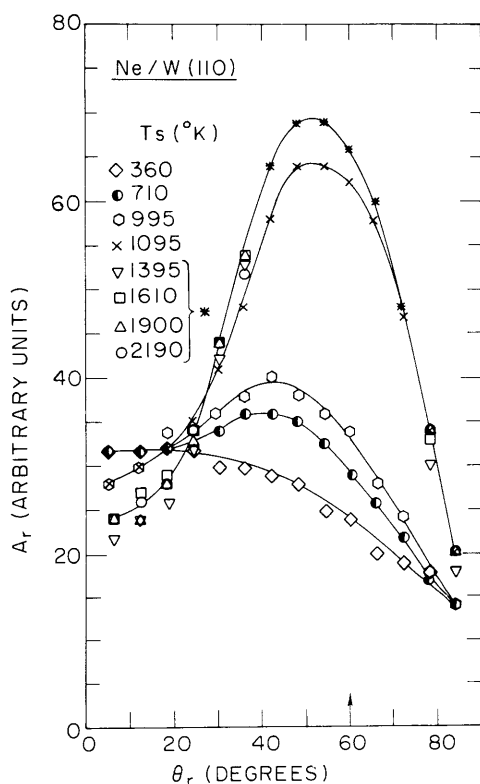The spatial distributions shown in Fig. XV-15 were measured for the scattering of Ne atoms of energy $E_i \approx 0.06$ eV and angle of incidence $\theta_i = 60°$ from the W(110) crystal at temperature T_s in the range 360-2190°K. The crystal had been thoroughly outgassed at $T_s \geqslant 2500°$K before this experiment, and it was flashed briefly to ~2200°K before measuring each distribution in Fig. XV-15. Since the residual gas pressure was nearly 1×10^{-8} Torr, however, the surface became recontaminated to some unknown degree during the time required to measure the spatial distribution at a given value of T_s, and this degree of contamination increases with decreasing T_s. The diffuse distribution observed for $T_s = 360°$K is consistent with the fact that at low temperature the surface will be covered by a rather random array of weakly bound species adsorbed upon a more strongly bound layer. The distribution becomes more lobular as T_s increases, most likely because the coverage of the weakly bound species decreases with increasing temperature. As we shall show, the drastic change in the distribution in going from 995°K to 1095°K appears to be the result of the desorption of CO from

Fig. XV-15.

Spatial distribution of Ne scattered from a W(110) crystal. Conditions: $E_i \cong 0.06$ eV, $\theta_i = 60°$, $360° \leqslant T_s \leqslant 2150°$K. Although the crystal surface is contaminated by residual gases at the lower values of T_s, it is expected to be atomically clean at 2150°K.

the surface. The only common contaminants that can exist on W(110) above 1095°K are oxygen and carbon, and the concentration of the latter species should be low because the target has been subjected to the standard procedure for removing carbon.[5] A surprising feature of Fig. XV-15 is that the distribution remains essentially constant as T_s increases from 1395°K to 2190°K, even though any oxygen adsorbed on the surface will desorb in this range,[5] thereby producing a change in the surface which should manifest itself as a change in the scattering distribution. On the basis of data to be presented below, we suggest that the amount of oxygen adsorbed on the surface was insignificant. It should be emphasized that, according to results obtained by LEED,[5] the W(100) surface should be _atomically clean_ at T_s = 2190°K, under the assumption that the crystal has been processed to remove carbon impurities from the bulk.

b. Scattering of Ne from W(110) with Adsorbed O_2

The results presented in Fig. XV-16 were obtained by intentionally contaminating the crystal surface with O_2 rather than with unknown residual gases. The crystal was flashed to ~2200°K, then held at ~400°K for 1 min in O_2 at 1×10^{-7} Torr, and, after allowing the pressure to return to the 10^{-9} Torr range, the spatial distributions shown in Fig. XV-16 were measured for increasing values of T_s. As in the preceding experiment, $E_i \approx 0.06$ eV and $\theta_i = 60°$. Notice that the distributions for $350° \leqslant T_s \leqslant 890°K$ are quite diffuse and essentially identical. A lobular distribution first appears at $T_s =$ 1000°K, and it grows monotonically as T_s increases. The distributions for $T_s \geqslant 1890°K$ are nearly identical to one another and to the distributions for $T_s \geqslant 1395°K$ in Fig. XV-15. Since the distributions in Figs. XV-15 and XV-16 differ substantially in the range $T_s \leqslant$ 1600°K, we conclude that the amount of O_2 in the residual gas is insignificant.

Since both T_s and oxygen coverage are varying simultaneously in the preceding experiment, a second experiment was performed in which spatial distributions were measured for constant T_s, with the coverage being varied from 1 monolayer to 0. The procedure was the following.

1. The crystal was heated to ~1270°K for ~30 min in O_2 at 1×10^{-7} Torr. (This specific value of T_s was chosen because it is sufficiently high to cause CO adsorption to be negligible but low enough to allow approximately a monolayer of O atoms to adsorb.)

2. While maintaining T_s constant at ~1270°K, the admission of O_2 was stopped and, after the chamber pressure dropped to the 10^{-9} Torr range, the Ne beam was introduced, and curve "A" in Fig. XV-17 was recorded.

3. The crystal was flashed to 1620°K for 30 sec, and curve "B" was recorded after T_s returned to ~1270°K. According to the LEED study of Germer and May,[5] a flash to ~1620°K will cause an ordered half-monolayer structure to form.

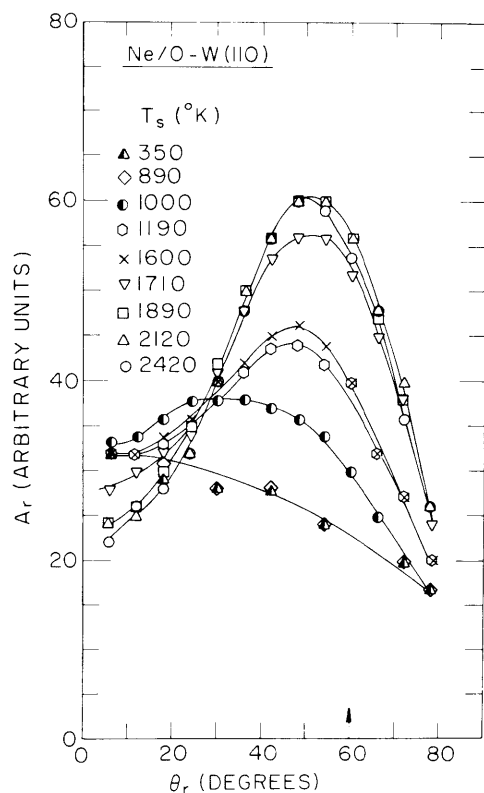4. The preceding step was repeated, but with the flash temperature increased to

Fig. XV-16.

Spatial distribution of Ne scattered from a W(110) crystal intentionally contaminated with O_2 before the measurements. Conditions: $E_i \cong 0.06$ eV, $\theta_i = 60°$, T_s increasing from 350-2420°K.
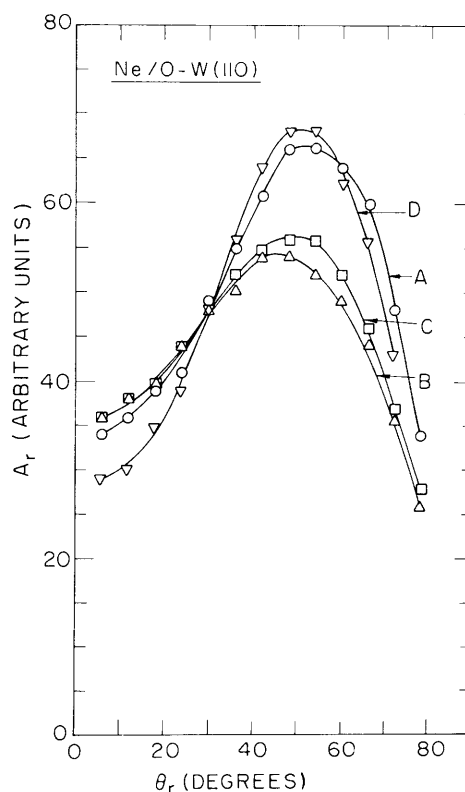
Fig. XV-17.

Spatial distribution of Ne scattered from a W(110) crystal with varying degree of oxygen coverage. Conditions: $E_i \cong 0.06$ eV, $\theta_i = 60°$, $T_s = 1270°K$. The crystal was flashed for 30 sec at 1620°, 1730°, and 2150°K between recording curves B, C, and D, respectively.

~1730°K, and curve "C" was recorded after T_s returned to ~1270°K.

5. The preceding step was repeated for a flash temperature of ~2150°K which is sufficient to desorb all oxygen from the surface.[5] Curve "D" was recorded after T_s returned to ~1270°K.

These results show that the spatial distributions do not vary monotonically with oxygen coverage at constant T_s.

c. Scattering of Ne from W(110) with Adsorbed CO

Since the results of experiments in which the crystal was intentionally contaminated with CO appear to be complicated by coadsorption of O_2, they will be repeated and then presented in a subsequent report. One interesting result of these experiments is included in Fig. XV-18, however, together with comparable results for

both "clean" and O_2-contaminated surface conditions. The curves labelled "CO" and "O_2" were obtained by flashing the crystal to ~2200°K, holding it at ~400°K for several minutes in CO or O_2 at 1×10^{-7} Torr and, after reducing the pressure to the
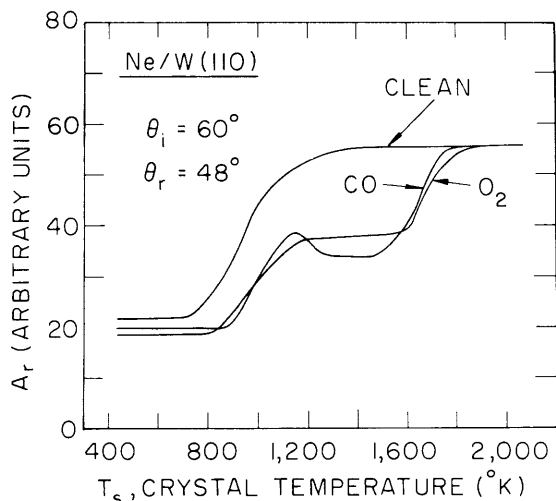

Fig. XV-18. Dependence of the scattered Ne signal at $\theta_r = 48°$ on crystal temperature, T_s, for a W(110) surface that was initially contaminated with CO, with O_2, or flashed "clean." Conditions: $E_i \cong 0.06$ eV, $\theta_i = 60°$.

10^{-9} Torr range, recording the detector signal at a fixed scattering angle ($\theta_r = 48°$) as T_s was increased from 400°K to 2100°K. The curve labelled "clean" was obtained by flashing the crystal to ~2200°K before each measurement so as to minimize the degree of contamination by residual gases. The principal features of Fig. XV-18 are (a) a maximum appears in the CO curve when T_s is approximately equal to 1100°K, the temperature at which the β state of CO desorbs from W(110),[6] and (b) the O_2 curve rises steeply when T_s approaches 2000°K, the temperature at which oxygen is completely desorbed from W(110).[5]

4. Concluding Remarks

These preliminary results demonstrate the sensitivity of LEMS to the presence of adsorbed species in the specific case of Ne scattered from W(110). A more thorough discussion of the results awaits completion of more extensive experiments that are now being performed. In these experiments the mean speed of the scattered atoms will be measured so that we can determine the degree to which energy transfer in gas-solid collisions depends upon the composition and structure of the adsorbate and/or crystal surface.

S. Yamamoto, R. E. Stickney

References

1. R. E. Stickney, in Proc. of 4th International Materials Symposium on "The Structure and Chemistry of Solid Surfaces," 1968 (in press).

2. J. N. Smith and H. Saltsburg, in Fundamentals of Gas-Surface Interactions, H. Saltsburg et al. (eds.) (Academic Press, Inc., New York, 1967), pp. 370-391.

3. R. E. Stickney, in Advances in Atomic and Molecular Physics, Vol. III, D. R. Bates and I. Estermann (eds.) (Academic Press, Inc., New York, 1967), pp. 143-204.

4. D. L. Smith and R. P. Merrill, in Rarefied Gas Dynamics, Proc. 6th International Symposium, L. Trilling and H. Wachman (eds.) (Academic Press, Inc., New York, 1968)(in press).

5. L. H. Germer and J. W. May, Surface Sci. 4, 452 (1966).

6. J. W. May and L. H. Germer, J. Chem. Phys. 44, 2895 (1966).

7. J. W. May, L. H. Germer, and C. C. Chang, J. Chem. Phys. 45, 2383 (1966).

8. S. Yamamoto and R. E. Stickney, Quarterly Progress Report No. 89, Research Laboratory of Electronics, M.I.T., April 15, 1968, pp. 49-56.

9. T. J. Lee, Quarterly Progress Report No. 91, Research Laboratory of Electronics, M.I.T., October 15, 1968, pp. 49-56.